Research Signpost
37/661 (2), Fort P.O.
Trivandrum-695 023
Kerala, India

Recent Developments in Wear Prevention, Friction and Lubrication, 2010: 263-278
ISBN: 978-81-308-0377-7 Editor: George K. Nikas

7. On the Stribeck curve

Michael M. Khonsari[1] and E. Richard Booser[2]
[1]*Dow Chemical Endowed Chair in Rotating Machinery, Louisiana State University, Department of Mechanical Engineering, Baton Rouge, LA 70803, USA;*
[2]*Engineering Consultant, Vero Beach, FL 32966, USA*

Abstract. Different regimes of lubrication in sliding at low surface speeds are often characterized by use of the so-called Stribeck curve. This chapter covers the changes in frictional processes encountered in passing from boundary lubrication at the start of motion, to mixed film lubrication at the lowest surface speeds, and finally to lift-off with development of a complete separating fluid film. Particular attention is given to analysis of asperity involvement in load support and friction in the mixed lubrication regime. In the final transition to complete lift-off, definition is also given to contributions by hydrodynamic fluid-film factors. Based on a historical perspective, related wear, wear-in, stick-slip, and lubricant additive effects are also reviewed.

1. Introduction

1.1. The Borromean rings

While this well-known design of three interlinked circles comes in many shapes and forms, importance of the structure is in its wholeness and unity: together the rings are inseparable, but the structure falls apart if any ring is detached. Within the context of tribology, each Borromean ring represents a major lubrication regime: boundary, mixed, and hydrodynamic (Fig. 1).

1.2. Lubricant regimes and tribological components

For many years, tribology researchers have focused on these individual regimes, with less attention to the whole structure. From one view point, this is not surprising: most applications involving conformal contacts – thrust bearings, journal bearings, hydrostatic bearings and the like – are primarily confined to the

Correspondence/Reprint request: Professor Michael M. Khonsari, Dow Chemical Endowed Chair in Rotating Machinery, Louisiana State University, Department of Mechanical Engineering, Baton Rouge, LA 70803, USA

hydrodynamic circle; while non-conformal applications – ball and roller element bearings, gears, and cam-followers – are concentrated contacts with surface asperity interactions belonging to the mixed lubrication ring, leaving the third ring to boundary lubrication.

Figure 1. The Borromean rings.

A tribological component, however, does not always operate in a single regime. Take a wet clutch in an automotive transmission, for example. It has a series of disks – alternating metallic separator disks and disks with porous and sand-paper-like friction material in close proximity in a bath of automatic transmission fluid (ATF).

At the onset of engagement, the clutch operates in the hydrodynamic regime, with the disk surfaces completely separated by ATF. The first stage of engagement begins when external pressure is applied to push the disks toward each other and hydrodynamic pressure is developed in the ATF as a result of squeeze action that supports most of the applied load. This period lasts only a fraction of a second, typically on the order of 0.01 s.

As the engagement process progresses, the disk separation gap drops and surface asperities come into direct contact with intimate interaction between disk surfaces. As the engagement continues, the film thickness is further reduced and so is the relative speed between the separator and friction disks. During this stage, the friction-lining material undergoes elastic deformation, as in the mixed lubrication regime, while the relative speed continues to drop.

Eventually, boundary lubrication prevails: relative speed between the disks becomes nil, and disks lock at the conclusion of the engagement. It follows, therefore, that in a full engagement cycle, the lubrication regime undergoes a transition from hydrodynamic, to elastohydrodynamic and mixed, and finally to

boundary lubrication – all within an engagement period lasting on the order of 1 second.

Clearly, therefore, the notion that a tribological component commonly works in any one regime does not hold. To understand the full extent of operating characteristics necessitates first-hand knowledge of all the lubrication regimes, i.e. the whole of the Borromean Rings and not an individual segment.

2. The origin and geniuses of Stribeck curve

The most interesting aspects and perhaps most challenging to predict are the processes that occur at interfaces between these three regimes. Further understanding of these transitions involves one of the most elementary concepts in the science of tribology: "the Stribeck curve" shown in Fig. 2.

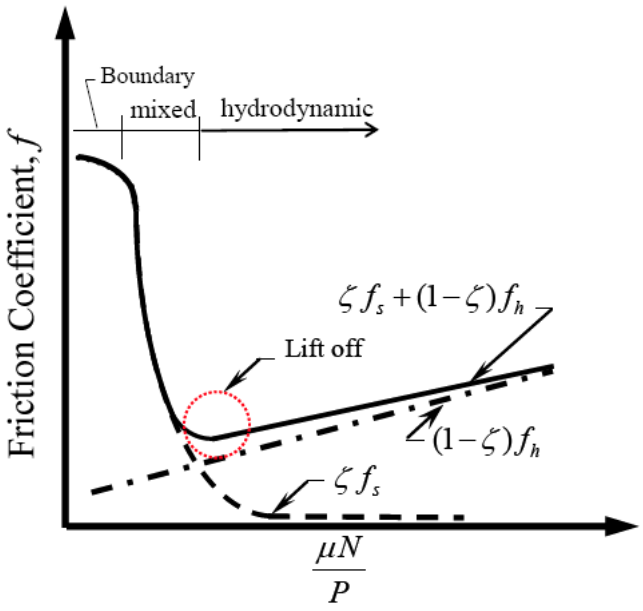

Figure 2. Illustration of the Stribeck curve.

The purpose of this article is not a historical perspective, nor a review of all relevant published papers. The interested reader can refer to Dowson [1] for the history and to Jacobson [2], Lu & Khonsari [3] as well as Wang *et al.* [4] for discussion on recent research developments and associated technical papers. Nonetheless, it is appropriate to relate the original work and discuss where current research seems to be heading.

In 1902, Richard Stribeck reported the results of a series of experimental tests conducted on a journal bearing [5] affirming that friction when plotted as a

function of speed gradually drops, passes through a minimum, and then increases. While the premise of this work trailed that of Hirn [6] by over half a century, the friction-speed characteristic is almost universally referred to as the Stribeck curve, in part due to the work of Gümbel [7] who summarized the results of Stribeck in a single curve.

There are several variations of Stribeck curve shown in Fig. 2. While the ordinate is always the coefficient of friction, the abscissa can be speed, Hersey number $\mu N/P$ – a dimensionless parameter akin to the Sommerfeld number S, which groups speed N [1/s], projected load P [N/m^2], viscosity μ [N·s/m^2], and the square of the inverted internal bearing clearance ratio (D/C_d or R/C_r)^2 – or the film parameter, Λ, which is film thickness divided by the composite surface roughness, $h/\sqrt{\sigma_1^2+\sigma_2^2}$. For thrust bearings, an analogous dimensionless number $K=\dfrac{\mu LU}{m^2W}$ may be defined, where $m=\dfrac{h_1-h_2}{B}$ with B representing the length of the slider bearing; h_1 and h_2 denoting the film thickness at the inlet and outlet of the slider, respectively.

Physically, one can postulate that the friction coefficient is a combination of two sources: the solid friction f_s and the viscous friction f_h expressed as follows.

$$f=\zeta f_s+(1-\zeta)f_h \tag{1}$$

where parameter ζ varies between 0 and 1 corresponding to fully hydrodynamic and dry friction, respectively.

As shown in Fig. 2, the Stribeck curve involves three distinctive features: (1) boundary lubrication at the left; mixed film lubrication where friction drops with increasing speed N up to a transition lift-off point; (2) a transition lift-off point where sufficient hydrodynamic fluid film pressure first develops with increased speed (higher S) to completely support the bearing load; and, finally, (3) a third zone having a complete separating fluid film with properties defined by viscous hydrodynamic behavior.

If load W is maintained constant in the hydrodynamic regime, increasing speed (or Sommerfeld number) translates to increasing film thickness h. Similarly, if the speed is maintained constant, increasing load results in a reduction in the film thickness, as one would intuitively expect. The following variations can be expected in this hydrodynamic regime where film thickness increase is generally proportional to the square root of speed over load:

- load-film thickness: $W \propto 1/h^2$,

- friction force: $F \propto 1/h$, and
- friction coefficient: $f = F/W \propto h$

where $\propto$ denotes proportionality.

It follows, then, that coefficient of friction in the hydrodynamic regime increases directly with factors that tend to increase the film thickness, e.g., speed, viscosity, and inversely with load. The Hersey or the Sommerfeld number lump all of these relations into a single dimensionless variable of the form $\mu N/P$. This direct proportionality prevails for fairly large operating speeds so long as the flow remains laminar. Changes in the behavior of friction coefficient are, however, expected during transition to turbulent flows.

3. Mixed lubrication regime

Mixed lubrication regime is the mode where both the hydrodynamics of the flow and the surface roughness actively play a role: the load is partially carried by the pressure generated in the fluid and partially by the asperities, so that the total load is a combination of the two:

$$W_T = W_h + W_A \tag{2}$$

Compared to hydrodynamic lubrication, this mixed lubrication regime is far more difficult to model, especially the boundary lubrication zone where viscous forces do not play a major role and friction coefficient generally remains constant. The film parameter becomes minute, surface asperities are in intimate contact, and influence of the lubricant and its additives involve details of molecular proportions. Nevertheless, recent analytical developments and experimental tests have provided significant insight into behavior in this regime.

Investigating efforts toward modeling and understanding the characteristics of mixed lubrication have captured the attention of many researchers since the 1970s. The interested reader may refer to papers by Christensen [8], Tallian [9], Johnson *et al.* [10], Tsao [11], Jacobson [12], Yamaguchi and Matsuoka [13], Spikes and Oliver [14], Spikes [15].

It what follows, we briefly describe the ideas put forward by Glenick and Schipper [16] and extended by Lu *et al.* [17] to mixed lubrication in conformal contacts. The underpinning idea here is the so-called load-sharing concept developed by Johnson *et al.* [10] to determine the contribution of the asperities and hydrodynamic both in terms of load-carrying capacity and friction force.

Letting γ_1 and γ_2 represent the scaling factors for hydrodynamic and asperities, the total load balance equation can be expressed as follows.

$$W_T = \frac{W_T}{\gamma_1} + \frac{W_T}{\gamma_2} \tag{3}$$

Or, simply:

$$1 = \frac{1}{\gamma_1} + \frac{1}{\gamma_2} \tag{4}$$

where γ_1 and γ_2 are two unknowns that depend on the surface characteristics and film thickness.

Similarly, the friction force is the sum of the hydrodynamic friction and the asperity interaction friction:

$$F_T = F_h + F_A \tag{5}$$

Once the friction force and the total load are determined, the friction coefficient can be easily calculated using:

$$f = \frac{F_T}{W_T} \tag{6}$$

The hydrodynamic friction (traction) force depends on the lubricant viscous behavior. That is:

$$F_h = \int_A \tau_h \, dA \tag{7}$$

where τ_h represents the fluid shear stress and A is the area. Therefore, the lubricant constitutive equation is needed to proceed. One must note, of course, that Newtonian assumption may not be applicable, particularly in the view of limiting shear stress associated with high pressure rheological behavior.

The friction force due to the asperity interaction can be evaluated using the following expression:

$$F_A = \sum_{i=1}^{N} \int_{A_{c_i}} \tau_{A_i} dA_{c_i} \tag{8}$$

where τ_{A_i} represents the shear stress associated with the contacting of a pair of asperities, A_c is the area of the asperities in contact, and N is the number of asperities involved.

The parameter τ_{A_i} can be conveniently related to the contacting asperity friction coefficient by noting that

$$\tau_{A_i} = f_{A_{c_i}} P_{c_i} \tag{9}$$

where P_{c_i} is the central contact pressure of an asperity pair, which can be estimated using, for example, the relationships developed by Greenwood and Williamson [18] given below.

$$p_{c_i} = \frac{2}{3} n\beta\sigma_s \sqrt{\frac{\sigma_s}{\beta}} E' F_{3/2}\left(\frac{h_c - d_d}{\sigma_s}\right) \tag{10}$$

where n, β, σ represent the parameters associated with density, average radius, and standard deviation of asperities, respectively. E′ is the equivalent modulus of elasticity, h_c denotes the film thickness, and d_d is the distance between mean plane passing through the asperity summits and the mean plane through the surface height, approximately $1.15\sigma_s$. The general function $F_{3/2}$ is defined as follows.

$$F_{3/2}\left(\frac{h(x)}{\sigma_s}\right) = \frac{1}{\sqrt{2\pi}} \int_{\frac{h(x)}{\sigma_s}}^{\infty} \left(s - \frac{h(x)}{\sigma_s}\right)^{\frac{3}{2}} e^{-\frac{1}{2}s^2} ds \tag{11}$$

The coefficient of friction between different asperity pairs is often uniform, so that substituting Eq. (9) into Eq. (8) yields the following expression of the total friction force due to summation of all asperities:

$$F_A = f_c \sum_{i=1}^{N} p_{c_i} dA_i \tag{12}$$

Friction factors f_c for lubricated contacts are rarely available in the literature since test results become distorted not only by the hydrodynamic lift associated with viscous effect of the lubricant at all but very slow speeds, but also by any surface films generated by oil additives. In general, lubricated friction factor for the soft Babbitt alloy in bearing liners running with a steel shaft will range from about 0.10 to 0.15 (as compared with 0.17 to 0.25 as a common starting coefficient of friction), bearing bronzes from 0.20 to 0.25, and steel-on-steel varies more widely from about 0.30 to 0.50.

Asperity contact pressure given in Eq. (10) can be further related to the maximum Hertzian pressure using expression developed by Gelinck and Schipper [19]. The result is:

$$\frac{2}{3}n\beta\sigma_s\sqrt{\frac{\sigma_s}{\beta}}E'F_{3/2}\left(\frac{h_c-d_d}{\sigma_s}\right)=p_h\left[1+\left(a_1 n'^{a_2}\sigma_s'^{a_3}W^{a_2-a_3}\right)^{a_4}\right]^{\frac{1}{a_4}} \tag{13}$$

Substituting $\frac{E'}{\gamma_2}$ for E', $\frac{F_T}{\gamma_2}$ for F_T, and $n\gamma_2$ for n into Eq. (13), yields the following dimensionless equation in terms of γ_2

$$\frac{2}{3}n'\sigma_s'\sqrt{\sigma_s'}F_T'F_{3/2}\left(\frac{h_c'-d_d'}{\sigma_s'}\right)=\left[1+\left(a_1 n'^{a_2}\sigma_s'^{a_3}W^{a_2-a_3}\gamma_2{}^{a_2}\right)^{a_4}\right]^{\frac{1}{a_4}}\frac{1}{\gamma_2} \tag{14}$$

where $n'=nR\sqrt{\beta R}$; $\sigma_s'=\frac{\sigma_s}{R}$; $F_T'=\sqrt{\frac{2\pi BR'E'}{F_T}}$; $d_d'=\frac{d_d}{R}$.

For line contact, the EHL film thickness equations involve the following dimensionless parameters:

- dimensionless load parameter: $w=\dfrac{W_T}{E'RB}$
- dimensionless speed parameter: $u=\dfrac{\mu_o U}{E'RB}$
- dimensionless material parameter: $G=\alpha E'$

For a specified load and speed, the central film thickness can be determined using an elastohydrodynamic (EHL) analysis or readily available film thickness equations for “smooth surfaces,” such as those developed by Moes [20].

$$h_c' u^{-\frac{1}{2}} = \left[(\gamma_1)^{\frac{s}{2}} \left(H_{RI}{}^{\frac{7}{3}} + (\gamma_1)^{-\frac{14}{15}} H_{EI}{}^{\frac{7}{3}} \right)^{\frac{3}{7}s} + (\gamma_1)^{-\frac{s}{2}} \left(H_{RP}{}^{-\frac{7}{2}} + H_{EP}{}^{-\frac{7}{2}} \right)^{-\frac{2}{7}s} \right]^{s^{-1}} (\gamma_1)^{\frac{1}{2}} \qquad (15)$$

where

$$s = \frac{1}{5}\left(7 + 8e^{\left(-2\gamma_1^{-\frac{2}{5}} \cdot \frac{H_{EI}}{H_{RI}} \right)} \right);\ H_{RI} = 3M^{-1};\ H_{EI} = 2.621M^{-\frac{1}{5}};\ H_{RP} = 1.287L^{\frac{2}{3}};$$

$$H_{EP} = 1.311M^{-\frac{1}{8}}L^{\frac{3}{4}};\ M = Wu^{-\frac{1}{2}},\ L = Gu^{\frac{1}{4}};\ H_c = h_c' u^{-\frac{1}{2}}, h_c' = \frac{h_c}{R}$$

Note that in above equation, Johnson's load-sharing concept has been introduced into the formulation by substituting E'/γ_1 for the equivalent modulus E' and W_T/γ_1 for the total load W_T.

Equations (4), (14) and (15) can be combined to determine h_c, γ_1 and γ_2. Then, Eq. (4) gives the total load W_T. The knowledge of h_c would enable computing the viscous friction and asperity friction in order to determine the total friction coefficient.

Figure 3 shows the results of simulations and experimental work of Lu *et al.* [17] for different oil inlet temperatures. This figure clearly indicates the usefulness of this modeling scheme for mixed lubrication. This concept was recently extended to analyze the lubrication behavior of grease-lubricated journal bearings [21]. There, the viscosity of the grease base oil was used to define a representative Sommerfeld number and a corresponding Stribeck curve for grease-lubricated bearings was developed. Remarkably, the mixed lubrication analysis prediction yielded good agreement with experimental measurements.

Extension of the mixed lubrication analysis to starved line contacts was made by Faraon and Schipper [22]. With this powerful tool, one can efficiently handle very difficult problems involving mixed lubrication with high degree of confidence. An application of this method to spur gears has been recently made by Akbarzadeh and Khonsari [23]. Gear surfaces are often several fold rougher than ball and roller element bearings and contact pressures are typically much higher than journal bearings. Further complications arise because the load and contact pressure change along the line of action during the engagements of gear teeth.

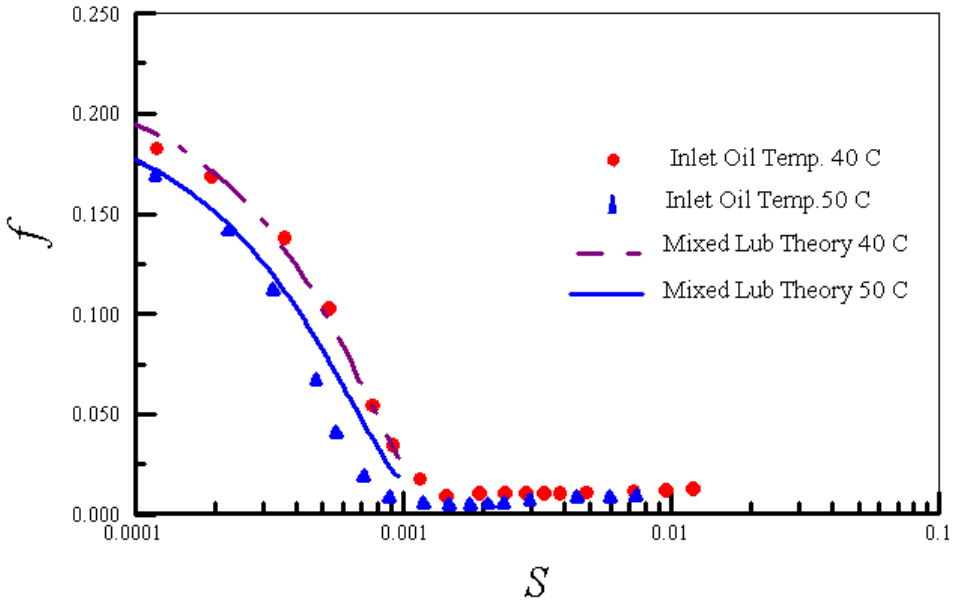

Figure 3. Comparison of predicted and measured friction coefficient as a function of Sommerfeld at two different oil temperatures [17].

In what follows, we confine our attention to applications involving journal bearings using approximate expressions that lend themselves to rapid estimation of the friction.

4. Application to journal bearings

4.1. Prediction of lift-off speed

As shown in the Stribeck curve, coefficient of friction reaches its minimum at the low oil-film thickness corresponding to the "lift-off" speed at which a full fluid supporting film first forms on start up. Above this speed, surface asperities have essentially no influence on friction; below lift-off speed, asperity peaks on the bearing and shaft surfaces begin to interact to restrain shaft motion with increased friction.

This lift-off speed can be observed in many electric motors and other rotating machines by monitoring their coast down. The otherwise steady pattern of deceleration from friction and windage is broken as friction increases when full-film support is first lost [24]. For a journal bearing, this transition speed N then will define the lift-off Sommerfeld Number ($S_o = \mu N/P(C_r/R)^2$) when including oil viscosity μ at the bearing temperature, radial load P, and clearance ratio (C_r/R), where C_r represents the radial clearance. With several bearings in question,

increase in load and lower viscosity (higher temperature or less viscous oil) may help define the results for an individual bearing.

Lift-off speed N_o can alternatively be calculated directly from Reynolds hydrodynamic equation modified as follows for low speeds and small oil film thickness h_o [3].

$$N_o = \left(\frac{h_o}{C_r}\right) P \left[4.678 \mu \left(\frac{R}{C_r}\right)^2 \left(\frac{L}{D}\right)^{1.044} \right]^{-1} \tag{16}$$

This h_o can be used with assumption that lift-off occurs when the ratio Λ of oil film thickness rises to 3 times the RMS journal finish, σ_j, when mating with a soft bearing surface commonly polished to a similar finish σ_b by initial operation. This corresponds to a composite film parameter at break-away $\Lambda = 3 = h_o/(\sigma_j^2 + \sigma_b^2)^{0.5}$. Asperity interaction can be expected as Λ drops below 3 and operation then enters the mixed film region of the Stribeck curve.

Equation (16) can be written in terms of the lift-off Sommerfeld number and the minimum film thickness, h_o[3]:

$$S_o = \frac{h_o}{4.678 C_r (L/D)^{1.044}} \tag{17}$$

where $h_o = \Lambda(\sigma_j^2 + \sigma_b^2)^{0.5}$. Note that Eq. (17) is derived by fitting an appropriate curve to the numerical results of Reynolds equation for a journal bearing operating under high eccentricity ratios. While Eq. (17) provides useful information, the prediction is only an estimate. Uncertainties arise as to polishing of asperities during the running in period.

Lubricant additives can also have a significant influence on the film thickness and corresponding lift-off speed. For example, experience with a lead Babbitt bearing surface loaded on a steel journal shows that 10 percent addition of sulfurized lard oil may increase the lubricant film thickness by two fold and at the same time reduce the friction coefficient by a third at lift-off. On the other hand, no effect on lift-off was obtained with a phosphate type anti-wear additive despite formation of a phosphate surface layer on the steel journal. Static coefficient of friction was 0.14 with both additives.

4.2. Extension to hydrodynamic operation

In hydrodynamic lubrication, the Reynolds equation provides a solution for the pressure and friction coefficient [25]. It is possible to develop an expression for a coefficient friction directly by appropriate curve fitting expression. Assuming that laminar flow prevails, the following expression can be derived for plane journal bearings [26].

$$f = (C_r / R)(0.43431 + \frac{0.33771}{(L/D)^2} + 19.32261S) \tag{18}$$

Equation (18) is best suited for eccentricity ratios in the range of $0.1<\varepsilon<0.9$. For very high eccentricity ratios, i.e. just after lift-off, Eq. (18) should be modified to read:

$$f = (C_r / R)\frac{1}{0.047932 \quad \frac{0.097555}{L/D} + \frac{0.13721}{\sqrt{S}}} \quad (0.9 \le \varepsilon \le 0.99) \tag{19}$$

This equation is valid for the eccentricity range of $0.9 \le \varepsilon \le 0.99$. For L/D =1, Eq. (18) should be valid for $S > 0.023$ and Eq. (19) for $S < 0.023$.

Figure 4 shows the prediction of friction coefficient using equations (18) and (19) along with numerical solutions of Reynolds equation over a wide range of Sommerfeld number. The results are indicative of the usefulness of these relations, particularly for journal bearings with aspect ratios of 1.

5. Related operating effects

The evolving definition of the Stribeck curve aids in understanding a variety of effects in bearings running at low speeds. The general performance map of Fig. 2 and the earlier discussion especially guides considerations of the following.

5.1. Higher friction

With operation at speeds below lift-off, friction typically rises by some 100-fold as rotation slows through the mixed-film zone. This translates into need for higher torque in a turning gear or other power source to maintain slow-speed rotation during cool-down or warm-up of a turbine, in creep speed of a ship or train, in

operations of heavily-loaded construction and earth-moving equipment, or in deep-drilling operations involved in oil and gas exploration where the rotational speed is typically below 200 rpm.

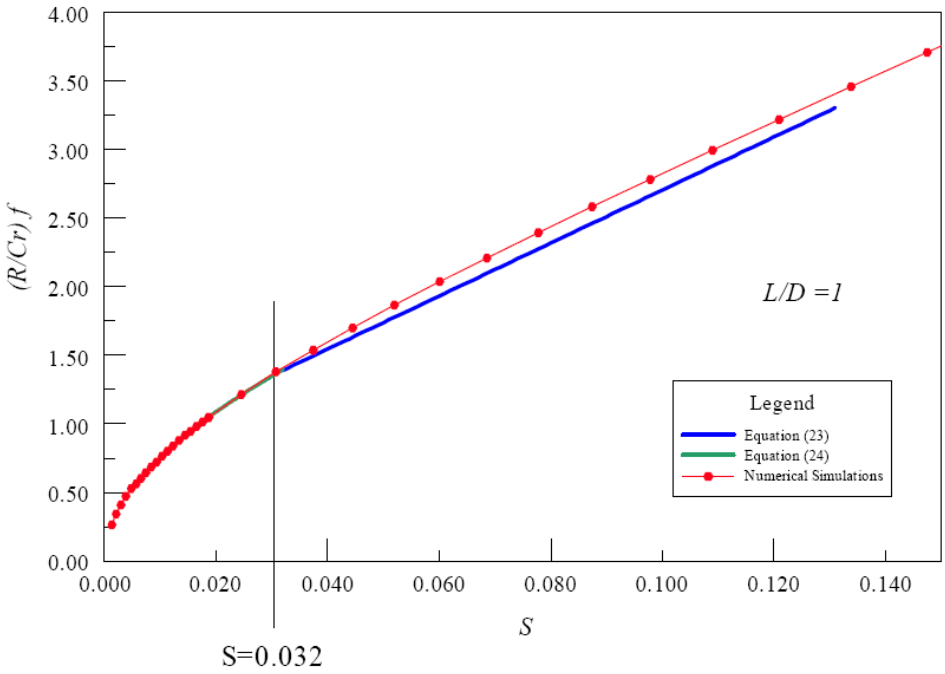

Figure 4. The behavior of friction coefficient in hydrodynamic regime.

5.2. Wear and wear-in

As more-and-more load is carried by metallic surface asperities at slowing speeds in the mixed lubrication zone, a proportionate increase is to be expected in wear rate. If design constraints permit, this deleterious effect can be reduced by applying higher lubricant viscosity, reducing contact unit load, or increasing rotation speed to lower the lift-off point. Use of antiwear and extreme-pressure lubricants may also reduce wear by forming protective surface layers on bearings.

Despite the general difficulty and uncertainty in predicting wear rates of asperity contacts, Maru and Tanaka [27] have demonstrated some relation of wear coefficients with friction coefficients, particularly in the beginning stages of the mixed-film regime.

Initial wear-in at mild operating conditions can provide a limited smoothing of the finish of both bearing and shaft surfaces. As shown in Fig. 5, this useful action moves the lift-off speed and the mixed lubrication region in the Stribeck curve to the left to reduce, or even possibly eliminate, the support needed from

contact of solid asperities [24]. Grease lubrication and some adhering oil-additive films produce a similar effect in lowering the lift-off speed.

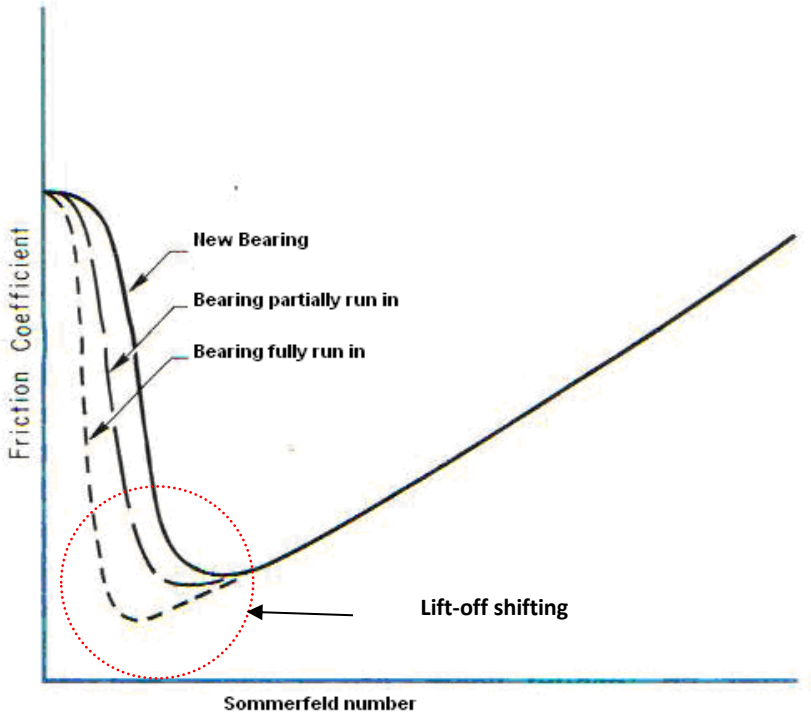

Figure 5. Behavior of Stribeck curve during the wearing in process (adapted from Elwell and Booser [24]).

5.3. Stick-slip chatter

When the shaft surface speed drops below lift-off, asperity peaks begin to interlace, and shaft rotation is restrained with the increased friction. If torsional elastic energy is then accumulated in a slowed or halted flexible shaft, it may then finally jump ahead. As the wind-up torque is then relieved, the shaft may stick again in a repeating stick-slip vibration or "chatter".

Long, limber shafts in turbines, compressors, oil-well drill shafts, and water-lubricated ship stern-tube bearings; and shaft face seals are susceptible to this chatter. A similar phenomenon may take place in satellite tracking devices swinging back and forth under ultra-slow speeds in ball bearings as they zero in on a target [28]. The hysteresis effects that are brought out by oscillatory motion—with a wide spectrum of amplitude, frequency, acceleration/deceleration effects that may be involved—add largely unexplored dimensions to the behavior of the classical Stribeck curve that await further research.

6. Concluding remarks

The Stribeck curve models low-speed bearing friction in two primary regions. On initial start-up in a mixed region, bearing load support by asperity contact is promptly supplemented by fluid film pressure that continually increases with increasing speed. When increasing speed finally generates sufficient oil film pressure to lift-off and support the total load, asperity contact is eliminated and a hydrodynamic region develops.

The mixed film region involves a complex pattern of load support involving wear and significantly higher friction. Asperity contact involved can be modeled by the Greenwood and Williamson [18] who formulated relations involving density, average radius and elastic modulus. Following lift-off into the hydrodynamic region, a direct expression is available for coefficient of friction from curve fitting of numerical solutions for Reynolds equation.

Accurate and reliable prediction of the performance of tribological components requires a systematic research strategy beyond focusing solely on the individual lubrication regimes. While the steady-state operation of many tribological components may dwell largely in a single lubrication regime, practically all machines go through entire the Stribeck curve when starting from rest. Henceforth, research should be devoted to the full spectrum of operating conditions. To this end, challenging questions remain to be at the interfaces between different lubrication regimes, from boundary to mixed and transition from there to hydrodynamic. This is an important step toward achieving the goals of virtual tribology design to provide the enabling computerized technology that minimizes expensive experimental testing.

Acknowledgements

The authors wish to thank the Drs. Lu, Jang, and Mr. Akbarzadeh (all from the LSU Center for Rotating Machinery) for their assistance and insightful discussion during the course of this investigation.

References

1. Dowson, D. 1998. *History of Tribology*, 2nd Edition, Professional Engineering Publishing, London and Bury St Edmunds, UK.
2. Jacobson, B. 2003. *Tribology International*, **36**, 781.
3. Lu, X., and Khonsari, M.M. 2005. *Tribology Letters*, **30**, 299.
4. Wang, Y., Wang, Q.J., Lin, Ch., and Shi, F. 2006. *Tribology Trans.*, **49**, 52.

5. Stribeck, R. 1902. Kugellager für beliebige Belastungen, Zeitschrift des Vereines deutscher Ingenieure, 46(37), 1341 (part I), 46(38), 1432 (part II), 46(39), 1463.
6. Hirn, G. 1854. *Bulletin of the Industrial Society of Mulhouse*, **26**, 188.
7. Gümbel, L. 1916. *Mbl. berl. BezVer. dt. Ing.* (VDI), 109.
8. Christensen, H. 1972. *Proc. Institution of Mechanical Engineers*, **186**, 421.
9. Tallian, T.E. 1972. *Wear*, **21**, 49.
10. Johnson, K.L., Greenwood, J.A., and Poon, S.Y. 1972. *Wear*, **19**, 91.
11. Tsao, Y.H. 1975. *Trans. ASLE*, **18**, 90.
12. Jacobson, B. 1990. *Wear*, **136**, 99.
13. Yamaguchi, A., and Matsuoka, H. 1992. *ASME J. Tribology*, **114**, 116.
14. Spikes, H.A. and Olver, A.V. 2003. *Lubrication Science*, **16**, 3.
15. Spikes, H.A. 1997. *Lubrication Science*, **9**, 2.
16. Gelinck, E.R.M., and Schipper, D.J. 1999. *ASME J. Tribology*, **121**, 449.
17. Lu, X., Khonsari, M.M., and Gelinck, E.R.M., 2006. *ASME J. Tribology*, **128**, 789.
18. Greenwood, J.A., and Williamson, J.B.P. 1966. *Proc. Royal Society of London A*, **295**, 300.
19. Gelinck, E.R.M., and Schipper, D.J. 2000. *Tribology International*, **33**, 175.
20. Moes, H. 1992. *Wear*, **159**, 57.
21. Lu, X., and Khonsari, M.M. 2007. *ASME J. Tribology*, **129**, 84.
22. Faraon, I.C., and Shipper, D.J. 2007. *ASME J. Tribology*, **129**, 181.
23. Akbarzadeh, S., and Khonsari, M.M. 2008. *ASME J. Tribology*, **130**, 021503.
24. Elwell, R.C., and Booser, E.R. 1972. *Machine Design*, issue 10, 129.
25. Khonsari, M.M., and Booser, E.R. 2008. *Applied Tribology – Bearing Design and Lubrication*, 2nd Edition, John Wiley & Sons, Inc, UK.
26. Jang, J.Y., and Khonsari, M.M. 2004. *J. Engineering Tribology*, **218**, 355.
27. Maru, M.M., and Tanaka, D.K. 2007. *J. Brazilian Soc. Mech. Sci. and Engrg.*, **29**, 55.
28. Khonsari, M.M., and Booser, E.R. 2008. *Machine Design*, issue 6, 80.